Lasers in Surgery and Medicine 19:177–183 (1996)

New Semiconductor Laser for Vitreoretinal Surgery

Claudio Azzolini, MD, Pier Giorgio Gobbi, PhD, Rosario Brancato, MD, Giuseppe Trabucchi, MD, and Marco Codenotti, MD

Department of Ophthalmology and Visual Sciences (C.A., R.B., G.T., M.C.) and Laser Medicine Research (P.G.G., R.B.), Scientific Institute H.S. Raffaele, University of Milan, 20132 Milan, Italy

Background and Objective: **We investigated the potential application in vitreoretinal surgery of a CW diode laser with cutting capabilities.**
Study Design/Materials and Methods: **A semiconductor CW laser emitting 300 mW optical power at 1.94 μm wavelength was used to perform retinotomies and membrane cutting on rabbit eyes. The device was integrated into a dedicated controller. The laser radiation was delivered through a low attenuation fused silica optical fiber of 200 μm core size, terminating into a 20-gauge endo-ocular handpiece. Histological aspects of threshold lesions obtained on the rabbits' chorioretina were evaluated by light microscopy.**
Results: **We obtained circular and linear full-thickness retinotomies with contact and noncontact procedures using energy of 120 mJ (240 mW × 0.5 s). Using a non-contact procedure, a larger peripheral coagulation halo around the retinotomies was observed, as compared to the contact method. The adjacent zone of thermal damage ranged from 50 to 200 μm. Lower efficacy was obtained on experimentally induced epiretinal membranes, where only superficial ablation was achieved.**
Conclusion: **The CW 2 μm diode laser will have a promising future in vitreoretinal surgery when a higher output irradiance is available.**

Key words: infrared laser, laser surgery, membranectomy, photoablation, retinotomy

INTRODUCTION

Vitreoretinal surgery requires instruments with high performance cutting capabilities in order to achieve peeling, delamination, and segmentation of different types of vitreoretinal membranes, as well as retinotomy and retinectomy. At the present time various kinds of mechanical scissors and picks in combination with vitreous substitutes are being used. In spite of careful surgery, it is not always possible to remove all membranes, and moreover unwanted retinal damage can occur.

The use of lasers with adequate cutting capabilities would allow the possibility of safer and extended tractionless removal of such membranes. In recent years experimental investigations have used different laser sources and wavelengths, as well as different interaction regimes. These studies include the needle-guided ArF excimer laser at 193 nm [1], the fiber guided XeCl at 308 nm [2,3], the transpupillary Q-switched Nd: YAG laser at 1,064 μm [4,5] (as an extension of the usual capsulotomy procedure), and a number of infrared emitting pulsed lasers with fiber guid-

Accepted for publication October 18, 1995.

Address reprint requests to Prof. R. Brancato, Dept. Ophthalmology and Visual Sciences, Scientific Institute H.S. Raffaele, University of Milano, Via Olgettina 60, 20132 Milano, Italy.

This report was presented in part at the Vitreoretinal Interfaces, October 27–29, 1994, San Francisco.

Fig. 1. View of the laser diode endocutter instrument complete with the optical delivery probe.

ing: the Ho:YAG laser at 2.12 μm [6], the Er:YAG laser at 2.94 μm [7–11], the CO_2 laser at 10.6 μm [12–14].

For the same purpose we focused our attention on the newly developed semiconductor lasers emitting continuous radiation in the wavelength region ~ 2 μm [15,16]. The aim was to test the microsurgical potentialities of such a laser source, characterized by compactness, good efficiency, high reliability, optical safety for the operator, and interesting perspectives for development.

MATERIALS AND METHODS

Laser Instrument

The laser source used for the present study is an SDL-6432-P2 laser diode (SDL, San Jose, CA), emitting up to 300 mW of optical power at 1.94 μm wavelength in continuous mode. The device is based on heterojunctions of quaternary semiconductors: InGaAsP/InP. The laser diode is provided with a fiber pigtail of 200 μm core diameter and 0.16 numerical aperture (NA), equivalent to a full divergence angle of 18°. The overall electrical to optical efficiency of the device is ~ 8%.

The laser diode was driven by a microprocessor controlled power supply, which was specifically developed in our laboratory. Output power levels were selectable with 10 mW resolution steps, and the pulse duration ranged from 10 ms to continuous emission. The instrument was operated with a footswitch, and its dimensions were 420 × 300 × 120 mm^3. The overall weight did not exceed 6 Kg (Fig. 1).

The laser radiation was delivered to the interaction site through a low-hydroxyl-fused silica optical fiber (for minimum absorption at this wavelength) of 200 μm diameter and 0.22 NA (25° full divergence). The connection between the fiber pigtail and the endolaser fiber was obtained by means of commercial connectors (SMA 905) resulting in an average power loss of ~ 20% (max power available at the fiber tip: 240 mW). The distal end of the probe was inserted and glued into a 20G needle attached to a handpiece.

Experimental Membranes

Three pigmented Dutch-belted rabbits with similar degree of pigmentation, with an average weight of 3.5 Kg, were used for this study. The research was conducted in compliance with the Association for Research in Vision and Ophthalmology (ARVO) Statement on the Use of Animals in Ophthalmic and Vision Research.

The animals were anaesthetized with i.m. injection of ketamine hydrochloride (0.5 ml/Kg). Proparacaine hydrochloride (0.5%) was administered for topical anesthesia. Tropicamide (1%) was applied for mydriasis.

The eyes were maintained in proptosis. A 25G surgical needle entered the vitreous cavity 4 mm posterior to the limbus without conjunctival incision. The needle was then advanced through the vitreous toward the retina and five to eight penetrations were made into the retina and choroid creating moderate vitreous bleedings. To allow the haemorrhage to expand, eye shaking was done. No suture was used to close the entrance site. Visualization was provided by indirect ophthalmoscopy. Tobramycin antibiotic medication was applied topically postoperatively and twice a day. Animals were examined by indirect ophthalmoscopy, and 2–3 weeks after the retinochoroidal punctures, elevated vitreous membranes were evident between the penetrations.

Laser Treatment

Surgery was performed using the same procedures for anaesthesia and pupil dilation already described. Under the operative microscope, a core and posterior vitrectomy was performed using an automated machine with suction and cutting capabilities (Optikon, Rome, Italy), injecting balanced salt citrate-buffered solution (BSS) (Alcon Surgical, Fort Worth, TX) through the infusion cannula.

Laser irradiation was performed from inside a half-filled eye bubble of perfluorodecalin (PFD) (DK-line, OPSIA, Ramonville, France), a low-vis-

cosity, high-density perfluorocarbon liquid injected into the eye. PFD was measured and found to be very transparent at the 1.94 μm wavelength, with an estimated absorption coefficient lower than 0.01 cm^{-1}. Diode laser cutting capabilities were tested on healthy retina and on experimentally induced membranes. Tests were performed both in contact with the tissue and at a distance of a few tenths of a millimeter from it. Color fundus photographs (Contax 139 Quartz, Japan) were taken. A drawing of the groups of laser spots was made immediately following the exposures to facilitate orientation for subsequent histopathologic correlation.

At the end of the surgical procedures, the animals were killed by a lethal dose of intravenous sodium tiopenthal while they were still deeply anaesthetized. The eyes were immediately enucleated and sectioned for macroscopic examination. The sections were maintained in a fixative solution of 2% glutaraldehyde in 0.1 molar phosphate buffer (PH 7.4) for 24 hours. The areas of impact were selected and postfixed in 1% osmium tetroxide solution in 0.2 molar cacodylate buffer. After the dehydration, the sectional pieces were embedded in epoxy resin. Thin sections were then cut with ultratome and stained with methylene blue.

RESULTS

Using a contact procedure, evident retinal holes with a modest white surrounding halo were obtained using energy of ~ 120 mJ (240 mW × 0.5 s) (Fig. 2). The retinal hole diameter is slightly larger (~ 300 μm) than the fiber core diameter; the hole is surrounded by a ~ 50-μm-wide blanched annulus. Retinal holes were more easily induced on detached retina. By irradiating at lower energies, we found the threshold for hole formation at ~ 80 mJ (Fig. 3). Under threshold, adhesion of the retina to the probe tip was sometimes observed. Extreme care was then necessary to avoid tractional retinal tears. We observed in these cases a reduced transmission of the probe, due to cellular debris deposited on its tip. Therefore, accurate cleaning of the probe tip was necessary to restore previous efficacy.

Using a noncontact procedure, with a probe tip-retina distance of < 0.5 mm, retinal holes were obtained with the same energy of 120 mJ. The hole size was smaller, surrounded by a white halo with an extension of 100–200 μm across, due to photocoagulation of the tissue by the wings of the divergent laser beam. Working at above-threshold energy, we did not observe any choroidal haemorrages.

Extended retinal incisions could be obtained with the continuous sliding of the probe onto the

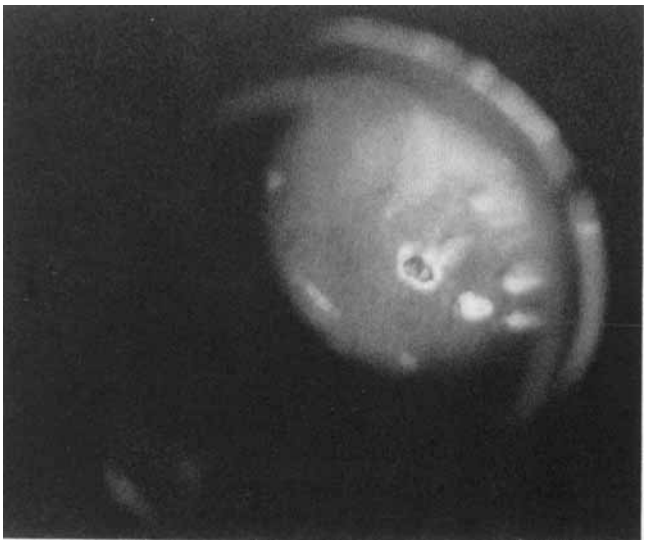

Fig. 2. Fundus photograph of a retinal hole obtained in contact mode, immediately following the irradiation. Incident energy was 120 mJ (240 mW in a 0.5 s pulse). The hole appears surrounded by other lesions obtained with separate subthreshold exposures.

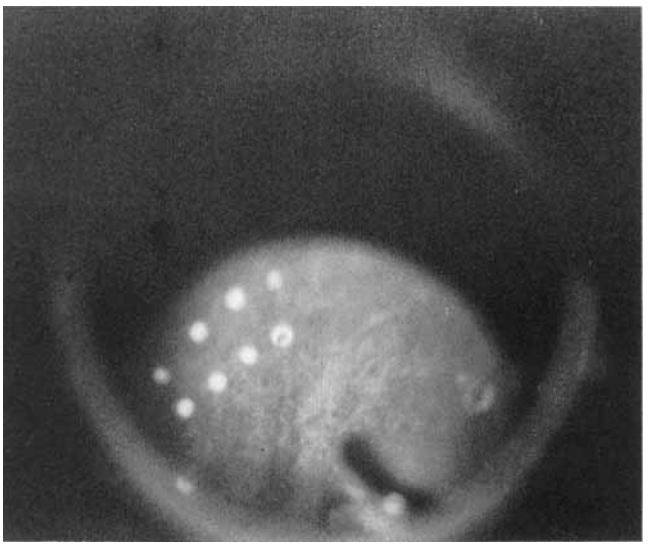

Fig. 3. Series of eight lesions produced on rabbit retina. A small retinal hole is visible inside the centermost lesion of the picture and was obtained in threshold conditions (200 mW × 0.4 s). All other lesions were obtained with progressively lower energy (power: 150–240 mW; exposure time: 0.1–0.4 s). They appear as very superficial photocoagulations.

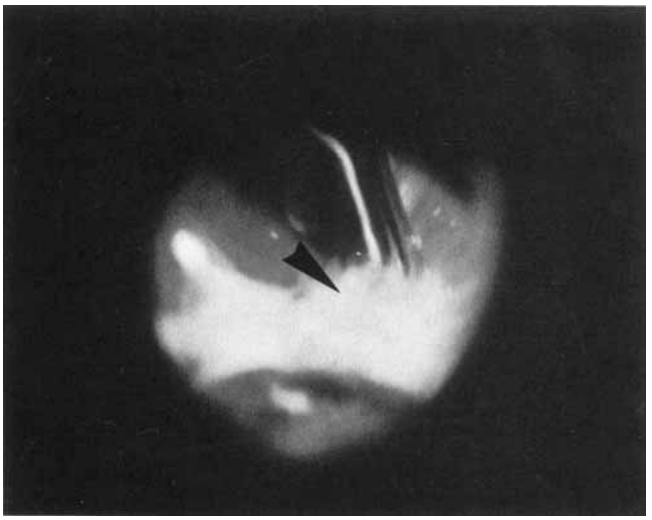

Fig. 4. Ablation of experimental vitreous membranes at 120 mJ/pulse. The 45° stainless steel tip of the laser probe (top) is placed in contact with a vitreous strand (bottom left). A cloud of ejected debris (arrow tip) hides the ablated zone.

Fig. 5. Photomicrograph of a retinal section showing a full thickness hole. Lateral thermal damage can be seen at the retinotomy edges. Damage to the underlying choroid is minimal. Due to sample preparation artifacts, retinotomy margins are averted and choroid appears separated from the retina (methylene blue, original magnification 400 ×).

retina, working at the smallest tip-to-retina distance to avoid traction (quasi-contact mode).

When irradiating experimentally induced epiretinal membranes, we observed ablation of the surface layers closer to the probe tip (Fig. 4). The maximum ablative effect was obtained irradiating at full power (240 mW) with 0.5–0.6 s exposures, resulting in an estimated thickness of the removed tissue of 40–60 μm per stroke. At same time, the deep membrane layers suffered mild shrinkage, which was secondary to thermal damage.

Complete transection of the robust membranes was difficult to achieve, because of the time length of the procedure (many tens of laser pulses) and due to the torsion and contraction movements of the fibrotic membrane, thus thwarting precise overlap of successive laser pulses onto the same target zone. Lengthening the laser pulse duration increased the thermal reaction of the tissue, without yielding an appreciable improvement in the ablation performance.

The histological study of the lesions in which the incision was ophthalmoscopically visible (Fig. 2) was characterized by thermal damage involving retinal tissue adjacent to the edges of the cut. In particular, all the retinal layers were thermally damaged along the borders of the incision. Some specimens showed retinal debris across the crater. The thermal damage was more pronounced in the areas close to the incisions, whereas at distances of 100–200 μm, it was characterized just by swelling phenomena of retinal layers. The study of the above-threshold lesions shows that minimal thermal damage involves the superficial choroidal layers as well (Fig. 5). No carbonization phenomena were observed.

DISCUSSION

Midinfrared Lasers

Surgical applications of mid infrared (MIR) lasers are essentially based upon the strong absorption exhibited by tissue water. At these wavelengths, in fact, there are no natural chromopores available for the optical interaction. Water has two main absorption peaks at 1.93 and 2.94 μm, where light can penetrate 80 and 1 μm in depth, respectively [17–19]. If an adequate amount of optical energy is delivered to such small layers of tissue penetrated by the infrared light, then vaporization of the water content is obtained together with decomposition of tissue constituents. This is the basis for photothermal incision and ablation effects.

In the following discussion, we consider for a comparison with the diode laser presented here only those lasers emitting in this spectral region, being moreover the most appealing candidates as cutting lasers for vitreoretinal surgery.

The Er:YAG laser emits at 2.94 μm, thus directly matching the main water absorption peak, and requires the minimum amount of energy to get water vaporization while causing the

minimum collateral tissue damage [20]. Due to the shallow penetration of its wavelength, the volume of ablated tissue is also very small, thus requiring high repetition rates for an effective cutting action. Furthermore, the use of Er:YAG is still handicapped by the difficulties in finding a practical delivery system for the efficient intraocular transmission of its energy. Fruitful efforts have been made in the recent past to overcome this technological drawback [9].

The Ho:YAG laser emits optical radiation at 2.12 μm wavelength, where penetration depth in water is ~ 400 μm and can be fairly well transmitted through commercially fused silica optical fibers with low OH^- content.

Both the Er:YAG and the Ho:YAG lasers demonstrated good effectiveness in obtaining transection of vitreous membranes as well as creation of retinotomies on animal models. A common complication observed with such lasers is the possibility of inducing thermal damage or haemorragic lesions to the retina through the vitreous, even when working at considerable distance (a few mm) from its surface. Due to the extremely high absorption experienced by MIR radiation in water, this kind of damage cannot be explained by direct optical irradiation of the damaged site. On the contrary, the effect is secondary to the complex hydrodynamics triggered by the fast vaporization of the irradiated vitreous volume. Very likely it is due to the onset of convective motion of superheated fluid (hot jets) or even to the high pressure transients following the creation and collapse of a cavitation bubble. As a means to avoid these undesirable effects, use of endo-ocular probes with mechanical shields in front of the tip has been suggested [6,7], thereby reducing the risk of axial damage to remote structures but also greatly reducing their efficacy and versatility as a surgical tool. The use of well transmitting vitreous substitute, as we did in this study, clearly circumvents this problem, leaving, however, the risk of retinal damage by direct optical irradiation.

Short and Long Pulse Interaction

A common feature of Er:YAG and Ho:YAG laser sources is the short duration of the optical pulse (typically 200–300 μs). In principle, if the laser pulse duration could be lengthened (maintaining the optical energy constant), this would progressively slow down the hydrodynamic evolution that takes place in the vitreous body or in any absorbing vitreous substitute. The consequent smoothing of pressure transients would, of course, decrease the volume of the region exposed to risk of secondary damage by hot fluid jets.

This represents one of the main arguments in favour of using the semiconductor diode lasing at 2 μm in continuous mode, besides its technical and ergonomic merits already outlined in the Introduction. Moreover in this laser family, the emission wavelength varies according to the composition of the diode substrate in the range 1.85–2.05 μm, so that it can be chosen to match exactly the wavelength of highest water absorption in this spectral region.

The relatively low power emission presently available from these laser sources, however, places some constraints on the practical interaction regimes that can be achieved. The starting point for a rough physical analysis is simply the estimate of the external energy E_v required to vaporize an ideal water volume reached by the radiation emitted from the fiber. With the given geometrical parameters (fiber radius: 100 μm; penetration depth: 90 μm; $\lambda = 1.94$ μm; NA: 0.22) one gets $E_v \approx 20$ mJ as the threshold for vaporization.

This estimate clearly is on the low side with respect to our experimental finding of 80 mJ for the ablation threshold. The main point is that this schematic model does not take into account the influence on the interaction process of the exposure time, i.e., the length of time in which the energy delivery to the tissue takes place. Actually the threshold energy for photovaporization is lower for shorter pulse durations, whereas at longer time scales thermal conduction is more effective in spreading the deposited heat out of the optical interaction volume, thus inducing stronger thermal alterations to collateral tissues.

The crossover between the two extreme regimes (very short or very long pulses) is governed by the thermal relaxation time t_R, a parameter that depends on the tissue properties, the wavelength used, and the size of the laser beam [21]. For the present case conditions, we numerically evaluated for t_R a value of 26 ms, i.e., a time duration that is 20 times shorter than the exposure lengths effectively used. This means that heat conduction has to be considered in the interaction process and that the volume of tissue heated during the laser pulse is certainly larger than the volume directly irradiated by the laser light.

To obtain a rough quantitative evaluation of this effect, we built a simple 3-D physical model based on the heat transport equation. Our nu-

merical simulations indicate that approximately twice as much optical energy is required to reach the vaporization threshold for a laser pulse duration equal to t_R. For longer time exposures, the multiplicative factor increases, up to ten times the no-conduction estimate. Accordingly, the region of thermal damage (i.e., the volume risen to a temperature greater than the coagulation threshold) can extend up to 200 μm beyond the edge of the laser irradiation volume. Such numerical findings are in satisfactory agreement with the experimental results reported above and offer a suitable basis for evaluating the interaction at higher laser fluences and shorter time durations.

Scaling to Higher Powers

The extent of the lateral damage observed in retinotomies as well as the low efficiency recorded in cutting epiretinal membranes explicitly suggest the need for higher laser power to improve microsurgery performances of the diode laser at 2 μm. For example, we evaluated that a tenfold increase of the optical fluence would allow to obtain the same ablation effects by decreasing the duration of the laser pulse by a factor > 20. In this way the value of the thermal relaxation time can be approached, and therefore the amount of lateral heat spread out of the irradiation volume is reduced. At the same time, as far as resection capability is concerned, a proportionally higher cutting speed can be achieved with a satisfactory ablation yield.

It must be noted that the technology of 2 μm diodes laser is presently capable of delivering a maximum power in the 1 W range, i.e., four times higher than what was available to perform this work. Substantial output improvements are however within the reach of this laser technology, as happened with the companion diode family at 800 nm, and are to be expected in the near future. The goal for the present applications would be to reach ~ 3 W of power.

It must be pointed out, however, that what is actually needed is an increase in the tissue irradiance (in terms of power per unit surface: W/cm^2), and this could be already achieved at the available power levels with some kind of optical concentration of the radiation. The possible solutions include: (1) use of two or more laser devices with suitable addition of their powers, (2) use of smaller size optic fibers (with sophisticated optical injection) or of ribbon fibers, (3) development of focusing fiber tips, (4) use of sapphire terminations. Work is in progress in our laboratory to explore these possibilities.

CONCLUSIONS

Within the limits of the animal model used, our study demonstrated the feasibility of using low power semiconductor lasers emitting at 2 μm wavelength in continous mode to produce full-thickness retinotomies. These laser sources exhibit very interesting technical properties, such as good electrical-to-optical conversion efficiency, small size, high reliability, and long lifetime. From a clinical point of view, the wavelength is highly absorbed by soft tissues, whereas the CW mode of emission can prevent the onset of fast thermo-mechanical transients within the irradiated volume.

The power output presently available limits the incision depth and the cutting speed that could be theoretically attainable at power levels of 2–3 W. Further studies on animals and humans will allow deeper comprehension of the efficacy of this new laser compared to other laser sources and to traditional surgical instruments.

REFERENCES

1. Lewis A, Palanker D, Hemo I, Pe'er J, Zauberman H. Microsurgery of the retina with a needle-guided 193-nm excimer laser. Invest Ophthalmol Vis Sci 1992; 33:2377–2381.
2. Pellin MJ, Williams GA, Young CE, Gruen DM, Peters MA. Endoexcimer laser intraocular ablative photodecomposition. Am J Ophthalmol (letter) 1985; 99:483–484.
3. Marshall J, Sliney DH. Endoexcimer laser intraocular ablative photodecomposition (letter). Am J Ophthalmol 1986; 101:130–131.
4. Puliafito CA, Wasson PJ, Steinert RF, Gragoudas ES. Neodymium-YAG laser surgery on experimental vitreous membranes. Arch Ophthalmol 1984; 102:843–847.
5. Haut J, Le Mer Y, Monin C, Moulin F, Colliac JP. Twenty-five cases of relaxing retinotomy using a nanosecond Nd Yag laser (Yag-retinotomy). Graefe's Arch Ophthalmol 1989; 227:312–314.
6. Borirakchanyavat S, Puliafito CA, Climan GH, Margolis TI, Galler EL. Holmium-YAG laser surgery on experimental vitreous membranes. Arch Ophthalmol 1991; 109:1605–1609.
7. Margolis TI, Farnath DA, Destro M, Puliafito CA. Erbium:YAG laser surgery on experimental vitreous membranes. Arch Ophthalmol 1989; 107:424–428.
8. D'Amico DJ, Moulton RS, Panagiotis G, Theodossiadis PG, Yarborough JM. Erbium:YAG laser photothermal retinal Ablation in enucleated rabbit eyes. Am J Ophthalmol 1994; 117:783–790.
9. Brazitikos PD, D'Amico D, Bernal MT, Walsh AW. Erbium-YAG laser surgery of the vitreous and retina. Ophthalmology 1995; 102:278–290.

10. Peyman GA, Katoh N. Effects of an erbium:YAG laser on ocular structures. Int Ophthalmol 1987; 10:245–253.
11. Tsubota K. Application of erbium:YAG laser in ocular ablation. Ophthalmolgica 1990; 200:117–122.
12. Meyers SM, Bonner RF, Rodrigues MM, Ballintine EJ. Phototransection of vitreal membranes with the carbon dioxide laser in rabbits. Ophthalmology 1983; 90:563–568.
13. Miller JB, Smith MR, Boyer DS. Miniaturized intraocular carbon dioxide laser photosurgical system for multiincision vitrectomy. Ophthalmology 1981; 88:440–442.
14. Mainster MA. Ophthalmic application of infrared lasers: Thermal considerations. Invest Ophthalmol Vis Sci 1979; 18:414–420.
15. Major JS Jr., Nam DW, Osinski JS, Welch DF. High-power 2.0 μm InGaAsP laser diodes. IEEE Photon Technol Lett 1993; 5:594–596.
16. Major JS Jr, Nam DW, Osinski JS, Welch DF. High-power single-mode 2.0 μm InGaAsP laser diodes. IEEE Photon Technol Lett 1993; 5:733–734.
17. Hale GM, Querry MR. Optical constants of water in the 200-nm to 200-μm wavelength region. Applied Optics 1973; 12:555–563.
18. Zolotarev VM, Mikhailov BA, Alperovich LI, Popov SI. Dispersion and absorption of liquid water in the infrared and radio regions of the spectrum. Opt Spectrosc 1969; 27:430–432.
19. Muller G, Dorschel K, Kar H. Biophysics of the photoablation process. Lasers Med Sci 1991; 6:241–254.
20. Walsh JT Jr, Flotte TJ, Deutsch TF. Er:YAG laser ablation of tissue: Effect of pulse duration and tissue type on thermal damage. Laser Surg Med 1989; 9:314–326.
21. van Gemert MJC, Welch AJ. Time constants in thermal laser medicine. Lasers Surg Med 1989; 9:405–421.